CHAPTER IV

EXPERIMENTAL STUDY OF ELECTROMECHANICAL EFFECT IN SAMPLES WITH FIXED BOUNDARY CONDITIONS

4.1 Introduction

In the previous chapter, we developed a theoretical model of the influence of electromechanical coupling on the director configuration in cholesteric samples with fixed boundary conditions. In the present chapter we describe some experiments on cholesteric mixtures taken in cells made of appropriately treated glass plates which provide rigid boundary conditions to the director.

4.2 Experiments on materials with negative dielectric anisotropy

A cell was prepared using two conducting glass plates pretreated to get a homogeneous alignment of the sample. It was filled with a nematic liquid crystal with a negative dielectric anisotropy ($\Delta\epsilon$) and positive conductivity anisotropy ($\Delta\sigma$), which was chiralised by adding a cholesteric dopant. When a DC electric field is applied between the conducting glass plates, the dielectric torque due to the field will favour

the director to be perpendicular to the field. On the other hand, as we discussed in the previous chapter, the electromechanical effect produces a non-uniform distortion of the profile of azimuthal angles. The non-uniform distortion changes sign with that of the electric field. This type of pure azimuthal distortion without any tilt deformation can be expected to occur provided we maintain the applied voltage to be below the threshold for electrohydrodynamic (EHD) instability.

It is well known that the EHD instability (see, for example, Chandrasekhar, 1977) arises in a nematic with negative $\Delta\epsilon$ and positive Aa. Space charges are formed under the action of an electric field in such a medium. The applied field beyond a threshold value exerts a force on the space charges which tends to set them in motion creating a macroscopic flow (Fig. 4.1). At the onset of instability the medium breaks up into a set of hydrodynamic rolls. The necessary condition for this instability to set in is that the director relaxation time T should be longer than the charge relaxation time τ, so that space charges have time to develop in the medium. The charge relaxation time is given by

$$\tau = \frac{\epsilon_{\|}}{4\pi\sigma_{\|}}$$

The director relaxation time is given by

$$T = \frac{\eta_B}{\left[K_{33}q^2 - (\Delta\epsilon\,\epsilon_\perp E^2)/(4\pi\,\epsilon_{\|})\right]} \tag{4.1}$$

where η_B is the bend viscosity coefficient, K_{33} is the bend elastic constant and q(= π/d) is the wavevector of the instability. From eqn. (4.1) T decreases with increase in E as $\Delta\epsilon < 0$. We get a restabilization threshold beyond which $T < \tau$. At voltages which are above the restabilisation voltage, the EHD instabilities cannot occur. In the following, we describe experiments in which the applied voltage is either below the threshold for EHD instability or above that for restabilisation.

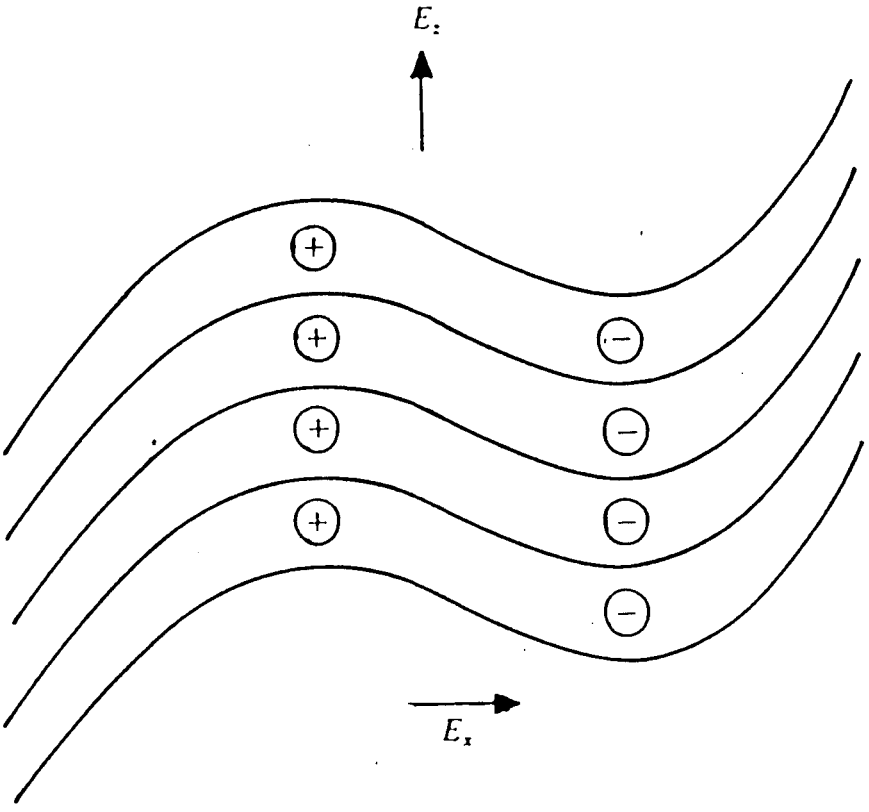

Figure 4.1. Space charge formation in an applied field E_z caused by a bend fluctuation of the director in a NLC with positive Aa.
E_x is the resulting transverse field.

We have used two techniques to look for the asymmetric director distortion produced by the electromechanical coupling in appropriately prepared samples.

4.2.1 Experiment using tiny cylindrical rods as microprobes

We used rods made of Quickfix, a commercial glue as microprobes. Quickfix can easily be drawn into fine, uniform rods. It can easily be cut into the required length as it hardens to some extent on exposure to air. Such thin, cylindrical rods of diameter $\approx 5\ \mu m$ were drawn and cured at $353K$ for about one hour so that quickfix polymerises and becomes harder. They were then cut to get rods of typical length of $\sim 25\ \mu m$.

Indium tin oxitlc coated conducting glass plates were treated to get a strong anchoring of the director by oblique evaporation of silicon monoxide at a grazing angle of $\sim 35°$ in a vacuum coating unit. Cells were prepared using stnall strips of mylar spacers of thickness $\approx$ **20** μm at the two edges of the coated glass plates. The exact thickness of the cell was measured using channelled spectrum.

We used a mixture ethoxyphenyl-trans-butylcyclohexyl carboxylate (EPBC) and methoxyphenyl-*trans*-pentyl cycloliexyl carboxylate (MPPC) in the ratio of **18** : 82 mole per cent with $\Delta\epsilon \approx$ -1, which was also used for the experiment described in chapter II. This nematic mixture of EPBC and MPPC was chiralised by adding 2.5 weight per cent of cholesteryl chloride. The structural formulae and transition temperatures of these compounds are shown in figure **4.2.** The pitch of the helix in this mixture was found to be $\approx$ **14** μm as measured by the Cano wedge technique. The cylindrical rods prepared as mentioned earlier were carefully inserted into the cholesteric sample taken in the cell. These rods floated in the sample as the density of the quickfix rods matched with that of the liquid crystalline mixture. The cell was

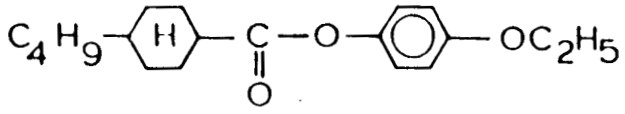

Ethoxy phenyl trans butyl cyclohexyl carboxylate

K 37 °C N 75 °C I

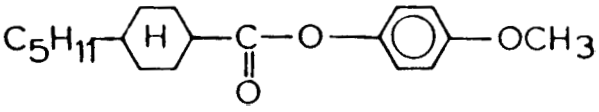

Methoxy phenyl trans pentyl cyclohexyl corboxylate

K 40 °C N 71 °C I

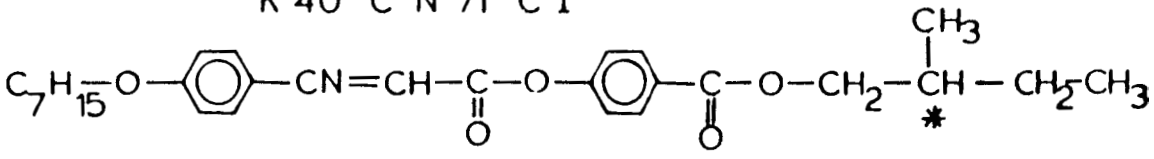

Methyl butyl benzoyloxy heptyloxy cinnamate

K 64 °C S_A 93 °A

63.5 °C

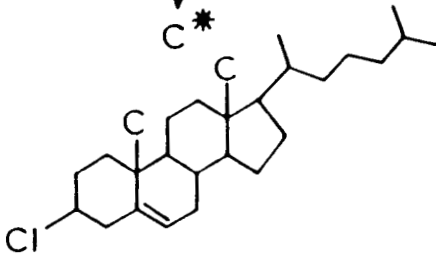

Cholesteryl chloride

K 97 °C I

62 °C

Cho

Figure 4.2. Structural formulae and transition temperatures of (1) EFBC, (2) MPPC, **(3)** C7, and (4) CC

observed between the crossed polarisers of a polarising microscope. A DC field of 5 volts which is well below the threshold for EHD instability in this mixture was applied across the cell. The orientation of the rod was found to change as the direction of the field was reversed. However, we also observed that tlie rod moved from one electrode to the other on changing the direction of the field. It always settled near the positively charged plate indicating that the rod was negatively charged. Comparing Fig.4.3a with Fig.4.3b, we can see that the rod is focussed differently for the two signs of the field because of its vertical motion. The orientation of the rod here represents the average orientation of the director close to the positively charged plate rather than the thickness averaged value. Therefore we did not attempt to calculate the value of the electromechanical coefficient by making quantitative observations on the movements of the rod. While moving from one electrode to the other the rod reorients with its long axis parallel to the local director. The experiment however brings out the physical mechanism of the electromechanical coupling, viz., the charged particles have a permeative helical motion in the cholesteric medium. This should, in turn, produce a torque on the director for conserving angular momentum.

4.2.2 **Experiment using the conoscopic technqiue**

Another method to study the variation of the average azimuthal angle of the distorted director field in a material with negative dielectric anisotropy is by using the conoscopic technique.

Conducting glass plates were treated to get a homogeneous alignment of the sample by the oblique evaporation of silicon monoxide. As we require relatively thick samples to get a conoscopic figure, cells of thickness $\approx 50\ \mu m$ were made using mylar spacers. The actual thickness of the cell was measured as usual using tlie

channelled spectrum.

We used 84 mole per cent of 2-cyano-4-heptyl phenyl-4'-pentyl-4-biphenyl carboxylate [7P(2CN)5BC] as one of the components of the mixture, as this material has a moderately high value of dielectric anisotropy $\Delta\epsilon \approx$-1.6 (Srikanta and Madhusudana, 1983) and 16 mole per cent of the optically active compound 4-cyano-4-(2-methyl) isobutoxy biphenyl (OA). The structural formulae of these materials are shown in figure 4.4. The pitch of the helix was measured by the Cano-Grandjean technique as described earlier and found to be $\approx 3.5\ \mu m$. The dielectric anisotropy of this mixture was estimated to be $\approx$ -1. The cell, filled with this mixture, was placed on the stage of a Leitz polarizing microscope between crossed polarisers. The sample was illuminated with light from a sodium lamp. The conoscopic observations were made by inserting a Bertrand lens in the path of the light beam.

We applied a low frequency (6 Hz) squarewave electric potential $\approx$ 210 volts between the ITO plates. As this is above the restabilisation voltage, the electrohydrodynamic instabilities are not produced in the sample as explained earlier. We get a conoscopic pattern which consists of two hyperbolic dark bands. It clearly rotated back and forth showing that the average value of $\bar{\phi}$ oscillates at the frequency of the applied field (Fig. 4.5).

According to de Gennes (1975), if 6 is the angle of rotation of the conoscopic figure,

$$\delta = \frac{1}{2} \tan^{-1} \left(\frac{\overline{\sin 2\phi}}{\overline{\cos 2\phi}} \right) \tag{4.2}$$

where ϕ is the azimuthal angle which is given by (see eqn. 3.3),

$$\phi(z) = \frac{\phi_d z}{d} + \frac{\nu_E E z(d-z)}{2K_{22}} \tag{4.3}$$

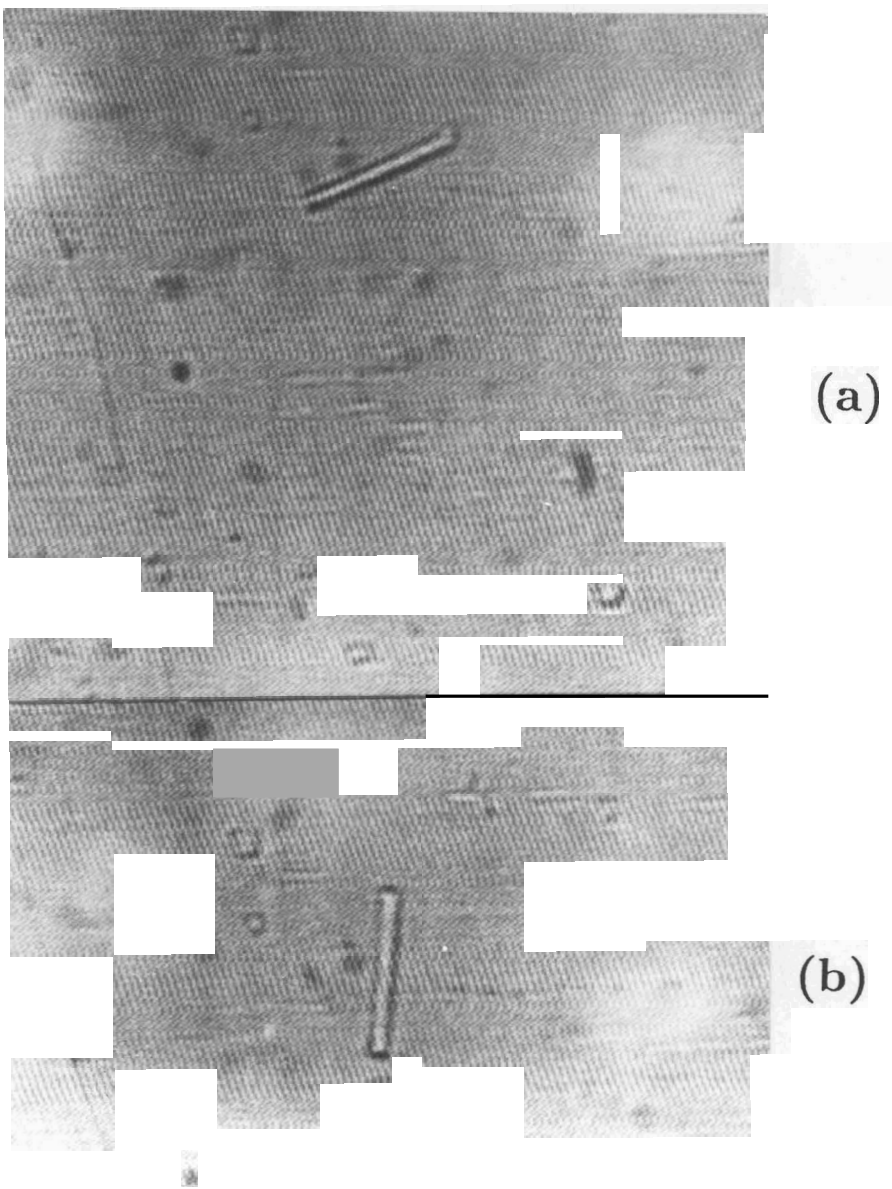

Figure 4.3. Print from a video recording showing the orientation of an epoxy rod in a cholesteric sample with $\Delta\epsilon \simeq$ -1, a twist of 3π radians and d=20 μm, as it settles close to the positive electrode. (a): + 5 V, (b) -5 V. The vertical motion of the rod causes the change in the focus (×500).

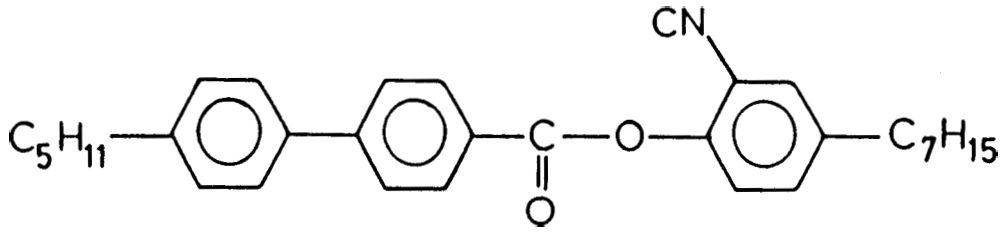

2 - cyano - 4 - heptylphenyl - 4′ - pentyl - 4 - biphenyl carboxylate

K 45.5 °C N 102 °C I

(1)

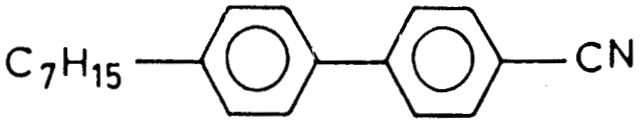

4 - n - heptyl - 4′ - cyanobiphenyl

K 28.5 °C N 42.1 °C I

(2)

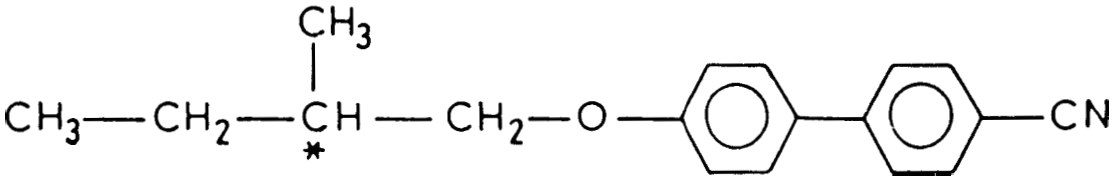

4 - cyano - 4′ - (2 - methyl) isobutoxy biphenyl

K 53.5 °C I

(3)

Figure 4.4. Structural formulae and transition temperatures of the compounds used in the experiment of section 4.2.2 (1) 7P(2CN)5BC, (2) 7CB, (3) OA.

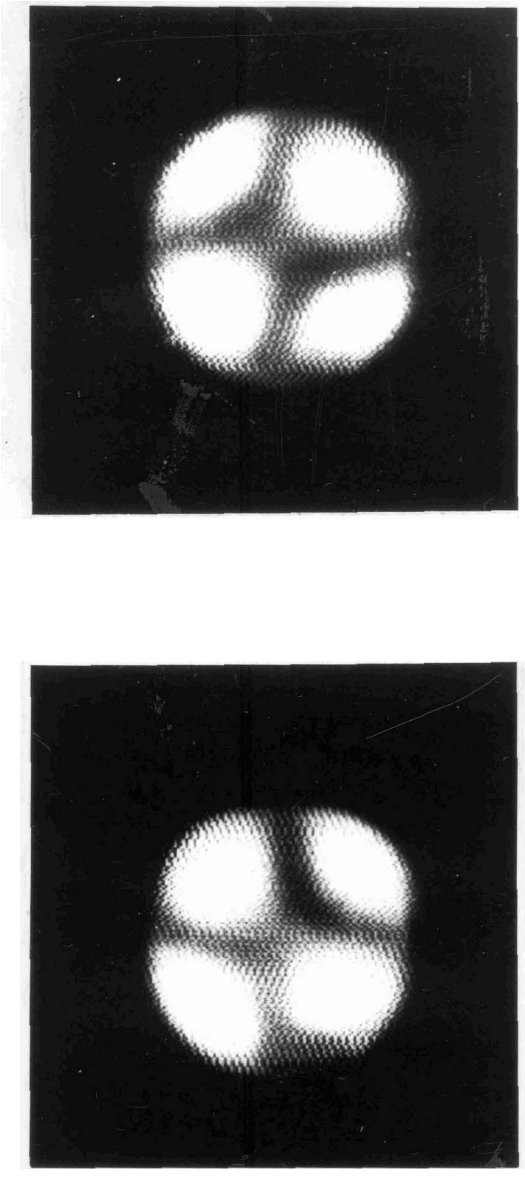

Figure 4.5. Print from a video recording showing the rotation of the conoscopic figures of a 50 μm thick negative $\Delta\epsilon$ material when the voltage oscillates between +210 V (left) and -210 V (right) at 6 Hz.

where $\phi = 0$ and ϕ_d at $z = 0$ and d respectively.

$$\overline{\sin 2\phi} = \frac{\int_o^d \sin 2\phi \, dz}{\int_o^d dz} \tag{4.4}$$

and

$$\overline{\cos 2\phi} = \frac{\int_o^d \cos 2\phi \, dz}{\int_o^d dz} \tag{4.5}$$

The integrals were calculated using Newton's method by dividing the sample thickness into 41 parts.

When the applied square wave voltage switched from +210 V to -210 V across the 50 μm thick sample, the conoscopic figure rotated by 1.66 radians. It rotated in the opposite direction by the same angle when the voltage was switched from -210 V to +210 V. We calculated the value of δ using equations (4.2) to (4.5). $K_{22} = 5 \times 10^{-11}$N, and $\phi_d = 29\,\pi radians$. The frequency of the square wave potential was quite low (6 IIz), and for the sake of simplicity we have assumed that the director configuration reached equilibrium, and we have ignored the viscous contribution to the torque in deriving equation (4.3).

From the experimental result of chapter II, $\frac{\nu_E}{q} \approx -2 \times 10^{-5}$ S.I. units. As the pitch P $\approx$ 3.5 μm in the present case, the value of ν_E was estimated to be $\approx$ 37 S.I. units. Using this value in equations (4.2) to (4.5), the calculated value of the change in the orientation of the conoscopic figure on switching the field from positive to negative value is $\approx$ 1.4 radians. This is comparable to the experimental value of $\simeq$ 1.66 radians.

Thus the value of the electromechanical coupling coefficient estimated by the conoscopic method is consistent with our earlier measurement of ν_E using cholesteric drops with free boundary conditions (chapter II).

4.3 Experiments on materials with positive dielectric anisotropy

As we have discussed in the previous chapter, we can overcome the Mauguin criterion by using a material with positive dielectric anisotropy because of the tilt-deformation of the director field above the Freedericksz threshold. But if $\Delta\epsilon$ is very large, the Freedericksz transition occurs at a very low voltage. The effect of electromechanical coupling becomes weaker as the average orientation of the director tilts towards the field as the voltage is gradually increased above the threshold (see equation **3.23).** Hence we selected a material with a relatively weak positive dielectric anisotropy in the hope of getting a reasonably strong electromechanical signal.

A mixture of **73** mole per cent of 7P(2CN)5BC and **27** mole per cent of 4'-n-heptyl-4-cyanobiphenyl (7CB) was prepared, the structural formulae of which are shown in Fig. **4.4.** The nematic phase of this mixture has a wide temperature range, between **45** and **90°C.** The dielectric anisotropy $\Delta\epsilon \simeq 0.2$ and the birefringence $\Delta n \approx$ **0.18** at **50°C** (Srikanta and Madhusudana, **1983).** Left handed cholesterics with the appropriate values of pitch were obtained by adding a few per cent of OA. Typically the pitch was $\simeq$ **10** μm and the sample thickness was $\simeq 3\mu m$ so that the director had a rotation of π radians in the sample. The cell was kept between the crossed polarizers of a polarising microscope. The sample orientation could be adjusted so that the direction of surface alignment makes an angle ψ lying between 0 and 90° with the substage polarizer. **A** photodiode (OSI-5K) was used to detect the optical signal. We used three different techniques to monitor the electrooptic signals due to the electromechanical effect in such samples.

In the preliminary observations, we recorded the electrooptic signal using a digital storage oscilloscope. At low enough frequencies of about a few Hertz, the medium

had a very clear linear electrooptic effect. As shown in figure 4.6, the signal varies at the frequency of the applied field when ψ=20°. On the other hand, the electrooptic signal oscillates at twice the frequency of the applied field when ψ is changed to 45°. This change over can be understood as follows.

The coefficient of transmitted intensity of a light beam passing through a homogeneously aligned nematic liquid crystal sample kept between two crossed polarizers is given by

$$T_1 = \frac{\sin^2 2\psi}{2}(1 - \cos \Delta\Phi) \tag{4.6}$$

where ψ is the angle made by the optic axis with the polariser and $\Delta\Phi$ is the phase difference between the extraordinary and ordinary rays passing through the sample. If the medium has a small change $\delta\psi$ in the azimuthal angle the change in the transmitted intensity is given by

$$\delta T_{I(\delta\psi)} = \sin 4\psi(1 - \cos \Delta\Phi)\delta\psi \ . \tag{4.7}$$

From this equation, it is clearly seen that the maximum in $\delta T_{I(\delta\psi)}$ occurs at $\psi = \pi/8$ radians. On the other hand, if there are θ variations which arise due to the dielectric anisotropy of the sample, $\Delta\Phi$ varies and

$$\delta T_{I(\delta\theta)} = \frac{\sin^2 2\psi}{2} \sin \Delta\Phi \, \delta(\Delta\Phi) \tag{4.8}$$

$\delta T_{I(\delta\theta)}$ has its maximum value for $\psi = \pi/4$ radians. The θ oscillations due to the dielectric coupling depend quadratically on the applied field and the corresponding time-dependent optical signal has twice the frequency of the AC field.

The electromechanical effect which is linear in E has no threshold. But as we have already discussed ϕ distortions can be made visible optically only when there is a sufficiently large θ distortion, i.e., above the Freedericksz threshold. This can be clearly seen by monitoring the optical signal on a spectrum analyser. For this

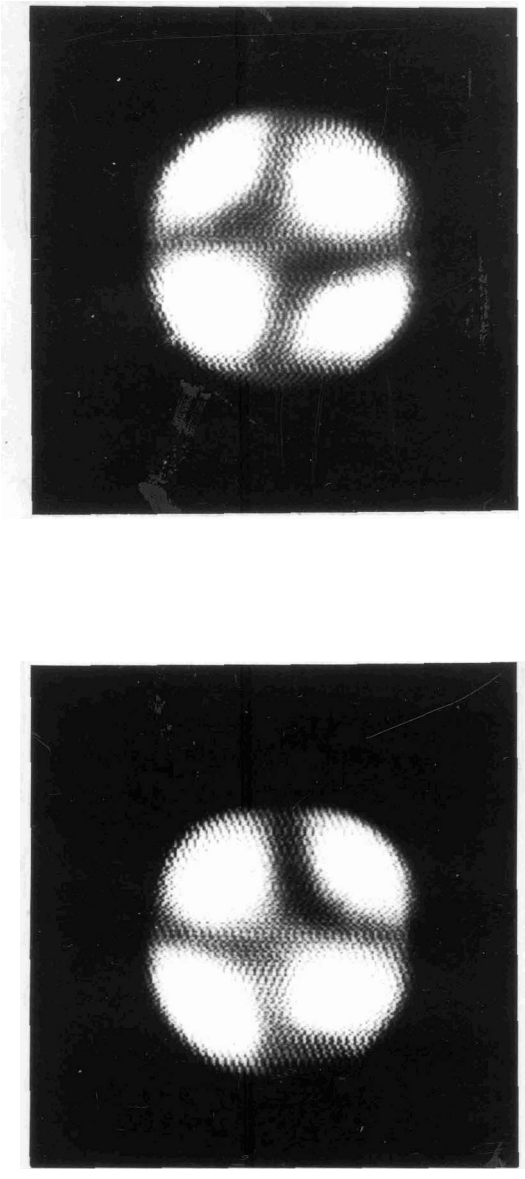

Figure 4.5. Print from a video recording showing the rotation of the conoscopic figures of a 50 μm thick negative $\Delta\epsilon$ material when the voltage oscillates between +210 V (left) and -210 V (right) at 6 Hz.

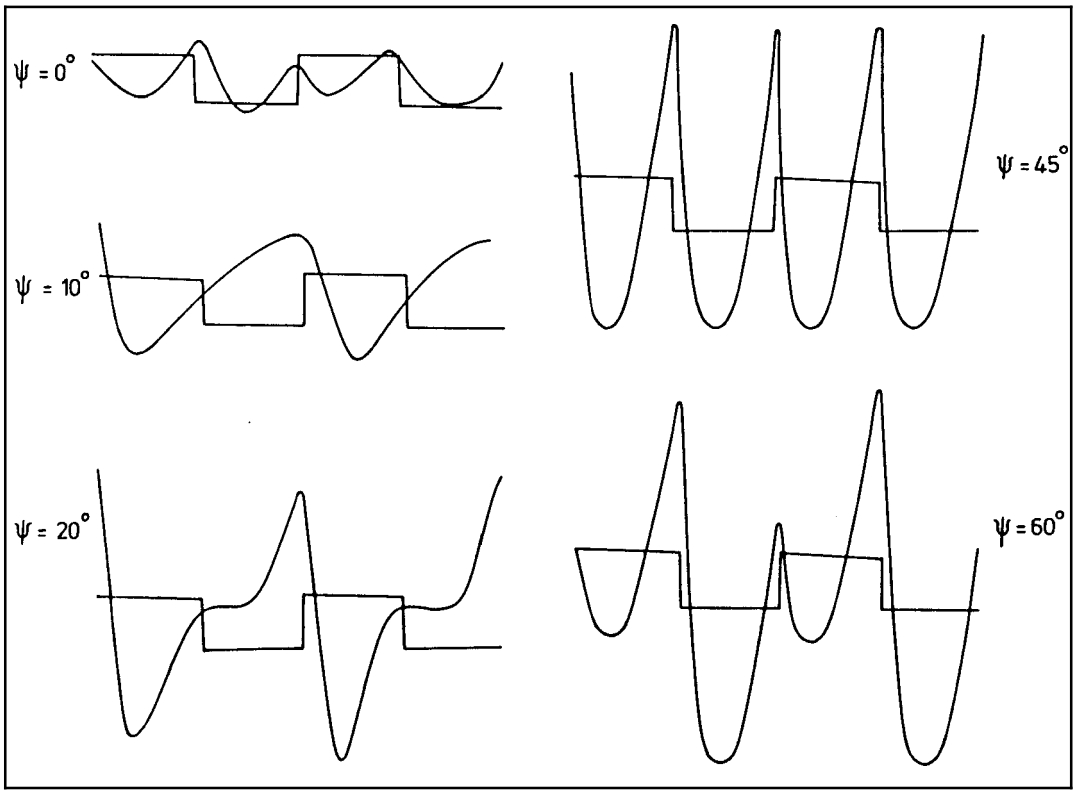

Figure 4.6. Electrooptic signal from a cholesteric with weak positive $\Delta\epsilon$ and subjected to a square wave voltage (of frequency 20 Hz and rms value 3 V), recorded from a digital storage oscilloscope after smoothening. ψ, the angle between the director on the bottom electrode and the polariser is varied between 0 and 60°. Notice the predominance of the f signal at $\psi = 20°$ and that of 2f signal at ψ=45°.

purpose, we used a cell of thickness $\approx 6\ \mu m$ filled with a mixture having tlic following composition. 73 mole per cent of 7P(2CN)5BC and 27 mole per cent of 7CB to which a small quantity of OA was added, to have a mixture with pitch $\approx 13\ \mu m$. The electrooptic signal was monitored using a spectrum analyser (Anritsu model No. MS420K). We applied a sinewave electric field to the sample at a frequency, say f. When we increased the applied voltage gradually, initially only the 2f signal developed, signifying a θ-distortion (Fig.4.7c). The f signal showed up at a slightly higher voltage as shown in figure 4.7d. When we increased the applied voltage further, we got a spectrum consisting of many higher harmonics indicating that the system became non-linear (Fig.4.7e-g).

We liavc made detailed quantitative measurements of the optical signals using a lock-in-amplifier (PAR model 5301A). The lock-in-amplifier facilitates both the field to be applied to the sample and the detection of f and 2f signals from the photodiode. Figure 4.8 shows a block diagram of the experimental set up. In this case the mixture consists of 81.3 mole per cent of 7P(2CN)5BC and 18.7 mole per cent of 7CB. A small quantity of OA was added to get a cholesteric mixture with pitch $\mathrm{P} = 18\mu m$. The sample was taken in a cell of thickness $\mathrm{d} = 3.2\ \mu m$ and was illuminated by a helium-neon laser beam. The electrooptic signals as functions of applied voltage at different frequencies are shown in figures 4.9 to 4.11. The 2 j signal shows the characteristic oscillations corresponding to a continuous decrease of the optical phase difference as the voltage is increased beyond the threshold. The f signal does not show such oscillations. Further, the f signal decreases continuously as the frequency is raised. This shows that the f signal arises from tlic electromechanical effect rather than the electroclinic effect (see Chapter V). Further, as we increased the frequency, the f and $2f$ signals become measurable at voltages which

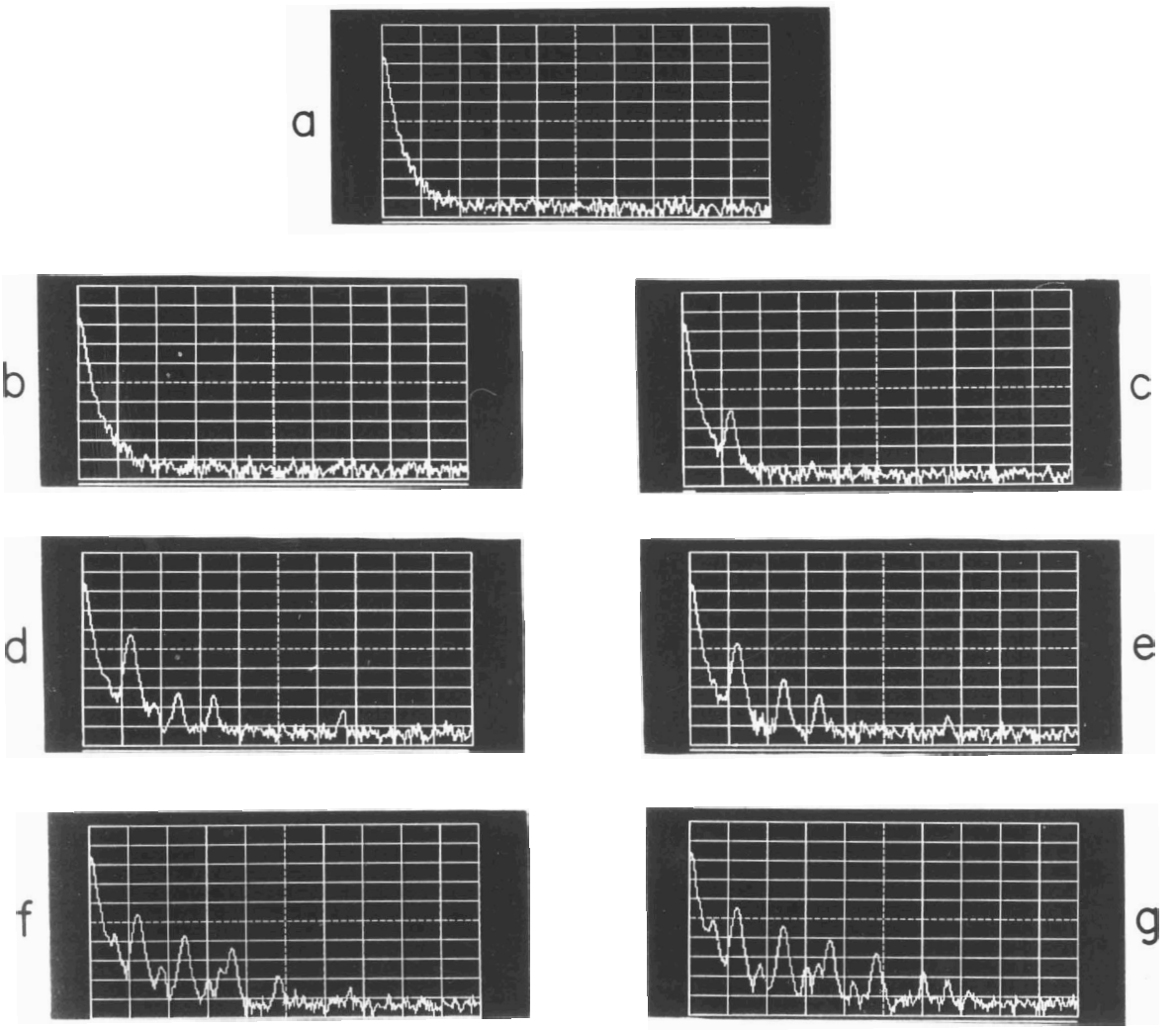

Figure 4.7. The spectrum of the electrooptical response of a chiral sample with **As** $\simeq +8$ with a a radian twist subjected to an 18 Hz sine wave electric field. $\psi \simeq 5°$. The rms values of the voltages are: (a) 0 V, (b) 1 V, (c) 1.5 V, (d) 1.8 V, (e) 2 V, (f) **3** V and (g) 4 V respectively. One horizontal division = 30 Hz.

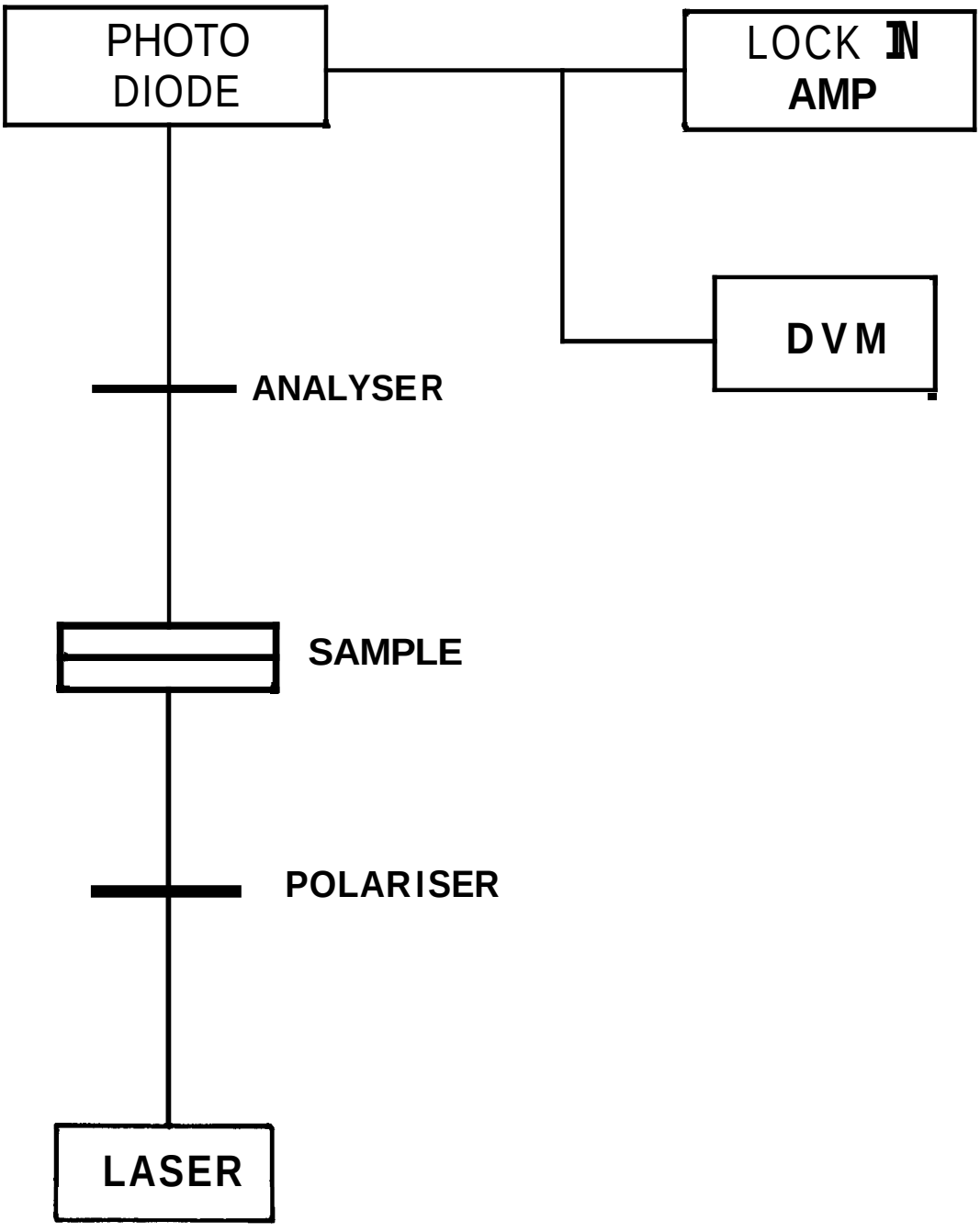

Figure 4.8. Block diagram of the experimental set-up to study f and 2f components of the electrooptic signal. The sample is kept on the rotating stage of a microscope.

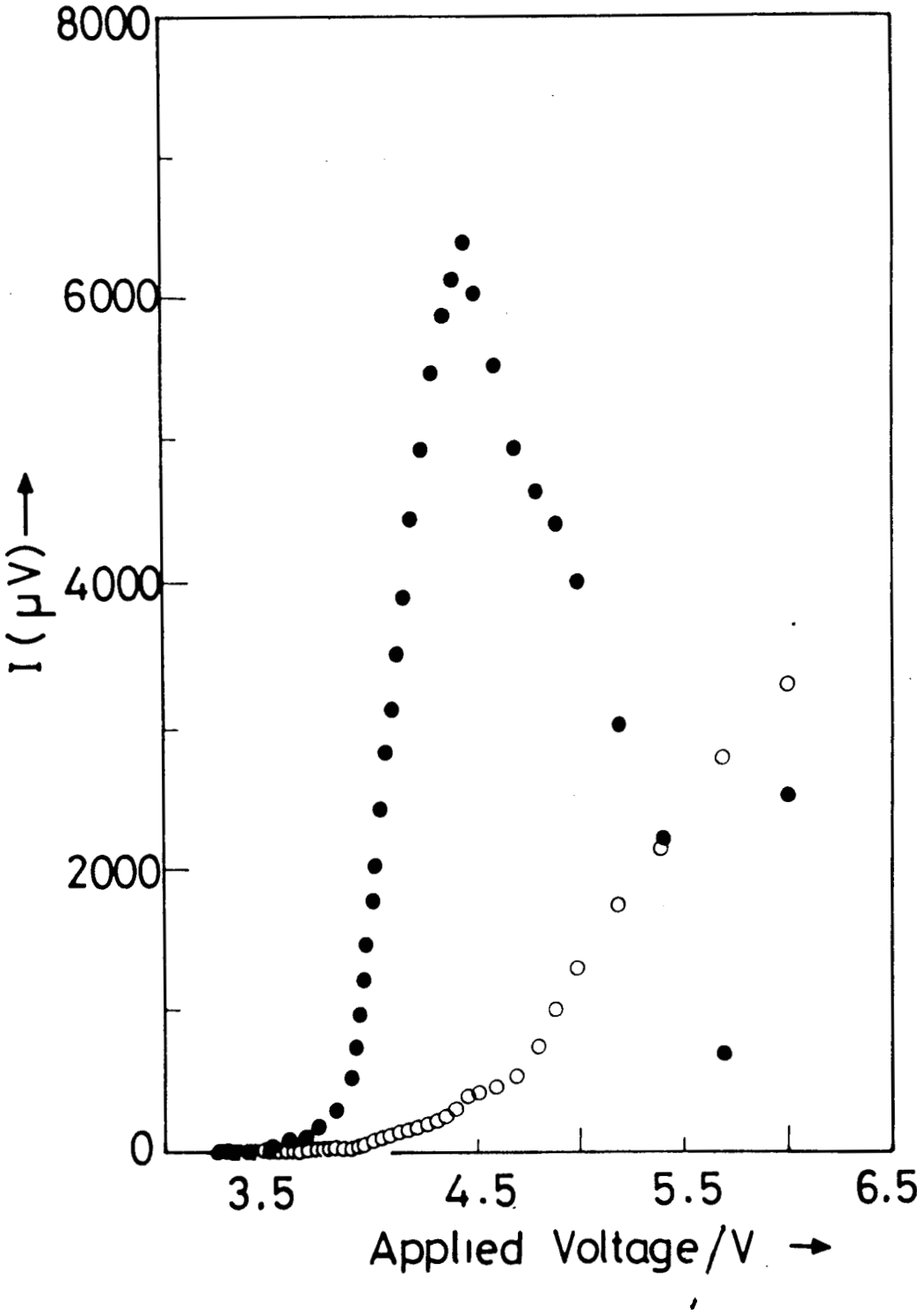

Figure 4.9. The f (open circles) and $2f$ (filled circles) components of the electrooptic signals from a **3.2** μm thick cholesteric sample with P=18 μm at $\psi=\pi/8$ radians, as functions of applied AC voltage at a frequency of 18 Hz.

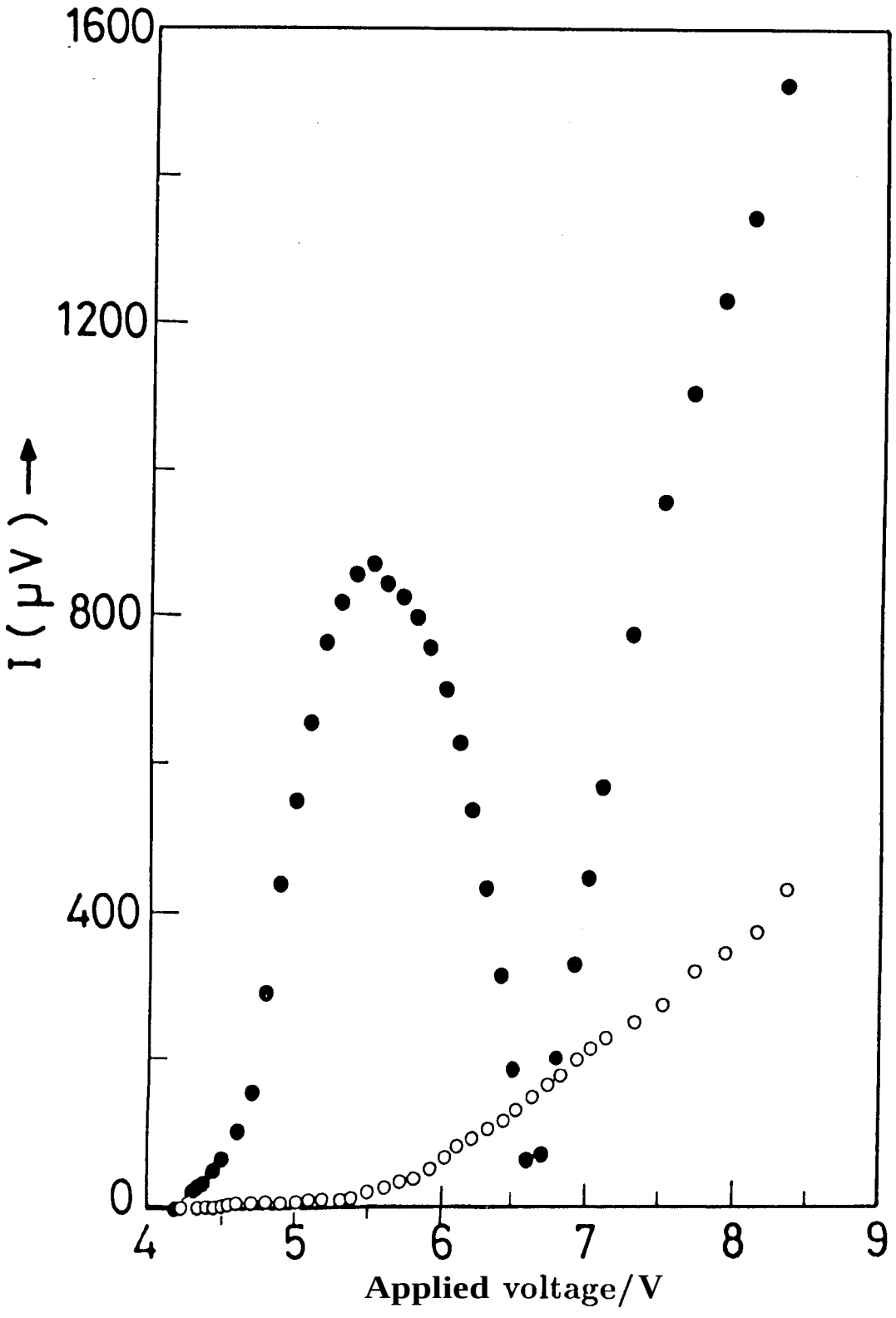

Figure 4.10. The f (open circles) and $2f$ (filled circles) components of the electrooptic signals as functions of applied AC voltage at a frequency of 171 Hz. The sample is same as in figure 4.9.

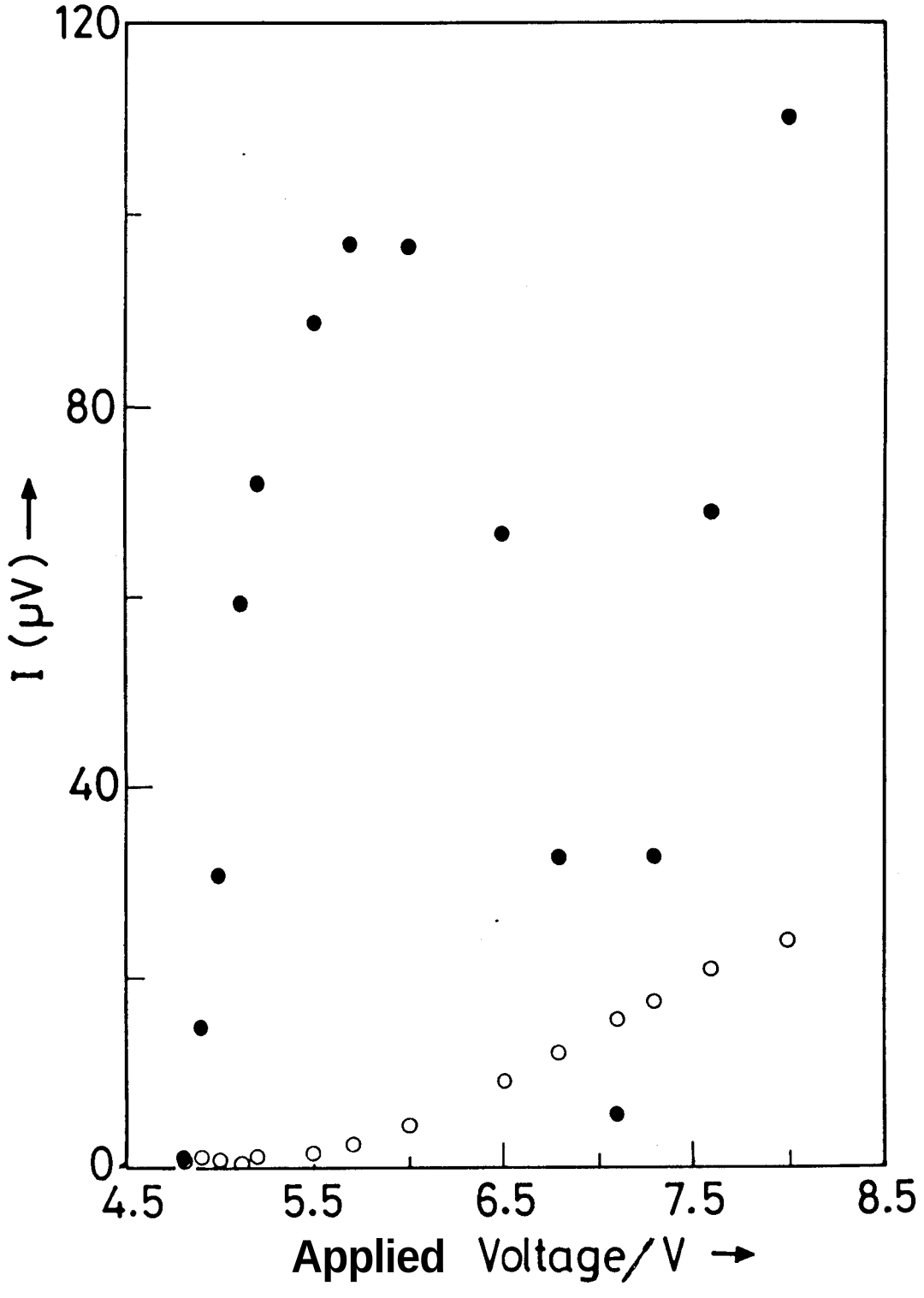

Figure 4.11. The f (open circles) and $2f$ (filled circles) components of the electrooptic signals as functions of applied AC voltage at a frequency of 1711 Hz. The sample is same as in figure 4.9.

are increasingly larger than the Freedericksz threshold. The sample is expected to have been untwisted as its thickness is less than $P/4$. In view of the linear dependence of ν_E on q that we found in our experiments on tlie drops (Chapter II) tlie present result indicates that ν_E depends on the natural wavevector $((2\pi/P)$ of the samples. We did a similar experiment on a 4.5 μm thick cell which contained the same mixture. There was a twist of $\sim 70°$ between the glass plates of the cell. In this case, the electrooptic signals (Fig.4.12) were found to be similar to those in figure 4.9, except that both the f and $2f$ signals were much stronger.

We also carried out an experiment with an unchiralised nematic mixture rnade of 84 mole per cent of 7P(2CN)5BC and 16 mole per cent of 7CB. The cell was constructed such that the rubbing direction of the upper plate oriented at an angle of $\sim 20°$ with respect to that of the lower plate. This results in an induced twist angle of $\sim$ 20" in the nematic director across the sample thickness which was $\approx 3\mu m$. This sample showed the ψ angle dependence of the f and 2f signals as shown in figure 4.13. The f signal again has a maximum at $\psi \simeq \frac{\pi}{8}$ radians and the 2f signal at $\psi \simeq \frac{\pi}{4}$ radians. The medium did not exhibit any striped domain pattern which is characteristic of flexoelectric distortions of tlie director (Bobylev et al., 1977) which can occur even with fixed boundary condition. Flexoelectric tilt distortions which are linear in E can also occur if the surface anchoring for tlie tilt angle θ is not strong enough. However, this process would have produced a peak of tlie f signal at $\psi = \pi/4$ radians. It would appear that there arc ϕ-oscillations in the sample and we believe that they are caused by the electromechanical coupling. When we twist a nematic, we induce a macroscopic chirality in the sample which has given rise to a non-zero value of the electromechanical coupling constant. Our observations in this experiment again show that the electromechanical coupling has

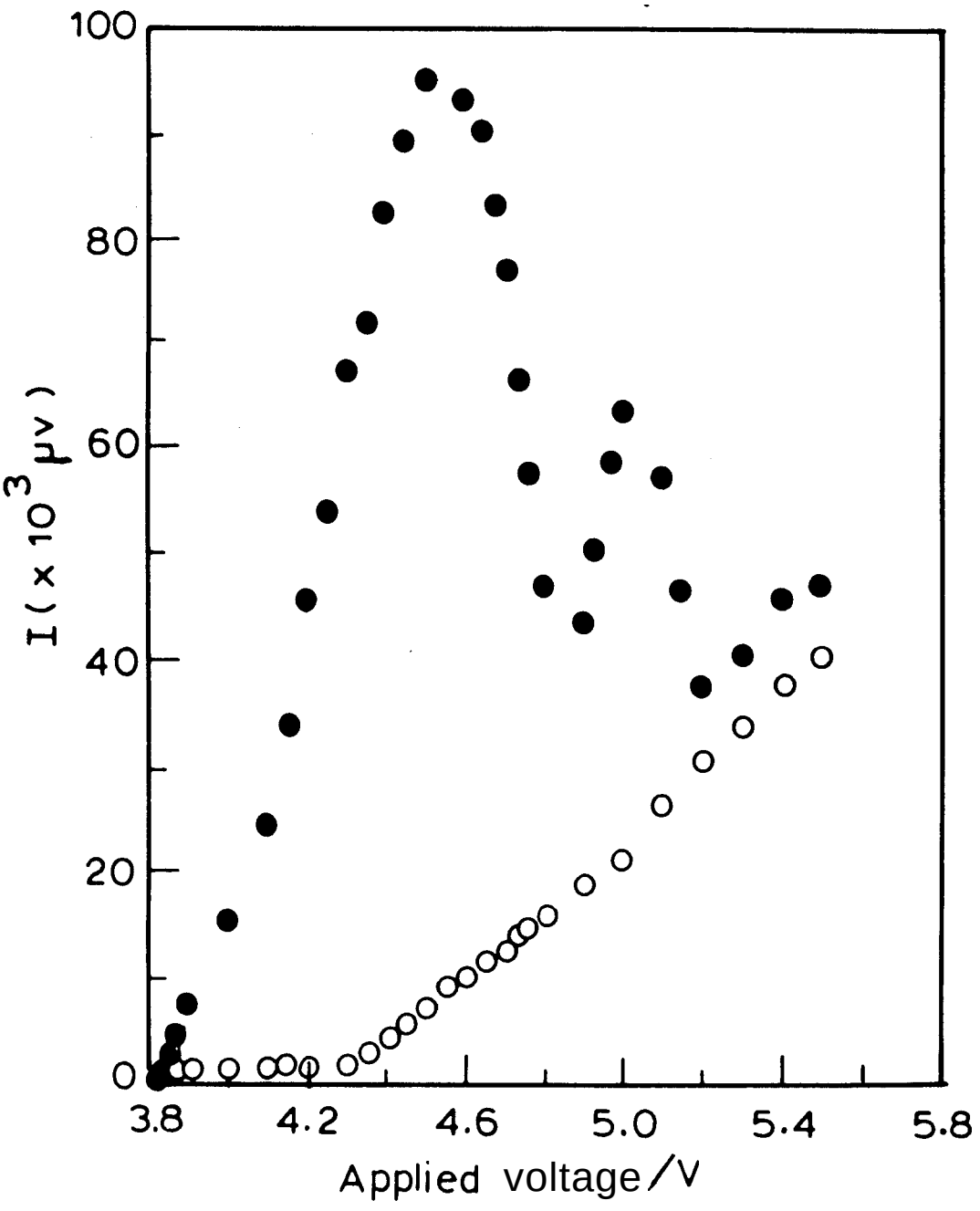

Figure 4.12. The f (open circles) and$2f$ (filled circles) components of the electrooptic signals from a 4.5 μm thick cholesteric sample with P=18 μm at $\psi=\pi/8$ radians as a function of applied AC voltage at a frequency of 18 Hz. There was a twist of 70° between the glass plates of the cell. Both f and $2f$ signals are significantly stronger than in the previous cell (Fig.4.9).

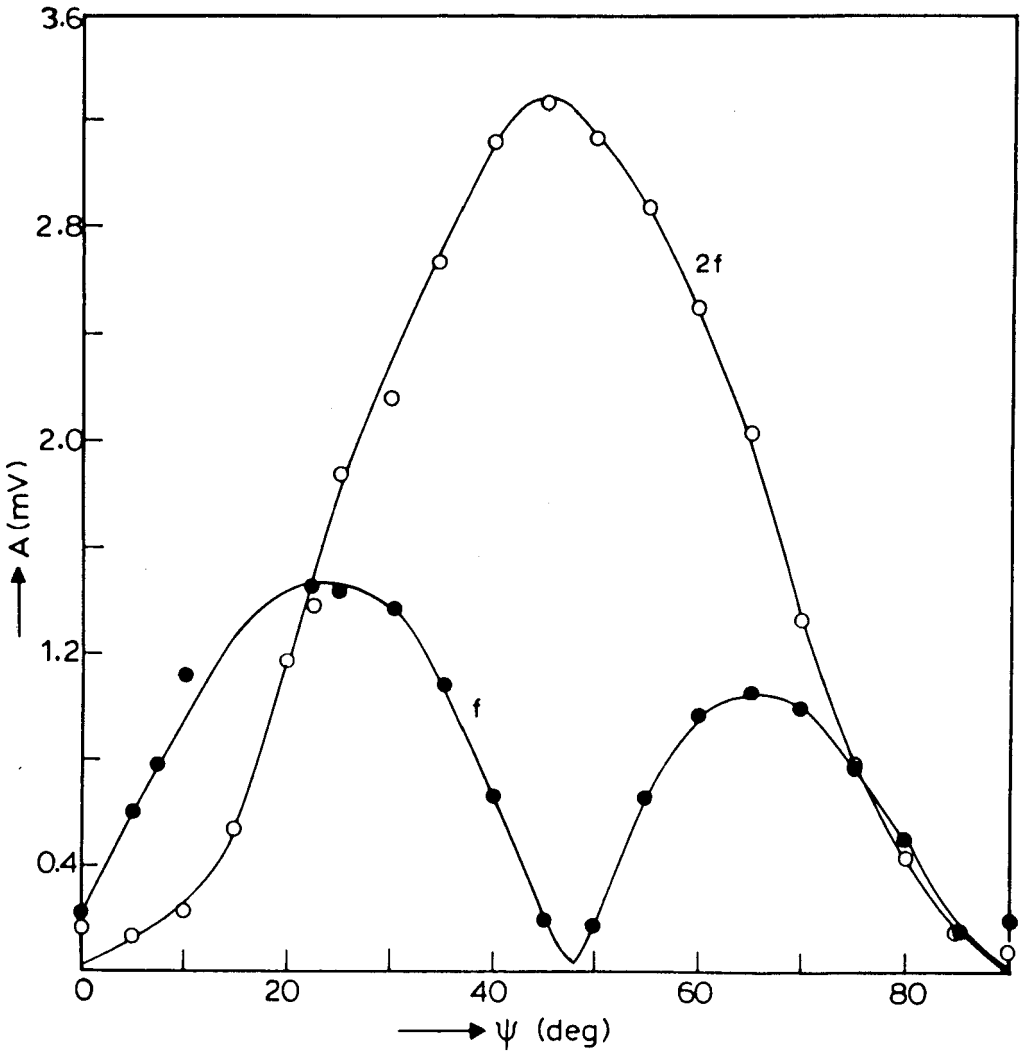

Figure 4.13. The ψ angle dependence of the f and $2f$ signals from a twisted nematic sample without any chiral component and with weak positive dielectric anisotropy. Twist angle = 20°, f = 18 Hz. The signals were amplified through the transformer input of the lock-in-amplifier.

a strong contribution from the macroscopic helical arrangement of the director.

We can point out here that Li et al. (1989, 1990) found a weak *electroclinic* effect (see chapter V) in the cholesteric phase of a system which shows a smectic A - cholesteric transition. They argued that a biaxial chiral molecule with a transverse permanent dipole could in principle give rise to an electroclinic effect. Since the electroclinic effect is essentially molecular in origin, it is practically insensitive to the frequency of the applied field in the range of 250 Hz - 10 KHz. On the other hand, as we have shown earlier, the electromechanical effect which is hydrodynamic in origin decreases quite rapidly with the frequency of the applied field. Morcovcr, tlie electromechanical effect is also exhibited in a twisted sample even though the molecules themselves are non-chiral.

4.3.1 Experiments on a compensated cholesteric mixture

As we have already discussed in chapter II, hydrodynamic theories assume that the electromechanical coupling coefficient ν_E depends on the macroscopic chirality of the system. Indeed the coupling coefficient ν_E is expected to change sign with that of the helix. This was confirmed in the experiments on cholesteric drops with free boundary conditions (Madhusudana and Pratibha, 1989). By adding different chiral cornpourids to a nematic liquid crystal, cliolesterics with different handedness can be obtained. Madhusudana and Pratibha showed in their experiment that when tlie handedness of the helix changes, the sense of rotation of the drops also changes. Further, as we have described in chapter II, we have made measurements of ν_E on cholesteric drops with different values of pitch. We have also used two chiral compounds with opposite handedness in suitable proportions to get a mixture with an infinite pitch. The drops did not rotate in this case showing that $\nu_E = 0$ in that

case. The graph of ν_E versus q (Fig.2.15) shows that tlie electromechanical coefficient varies linearly with q, passing through the origin as required by the hydrodynamic theories. As the concentration of chiral components is low in these mixtures, the influence of molecular chirality if any on the electromechanical coupling coefficient may be relatively weak. In the present section we report our experiments on a sample with fixed boundary conditions in which a compensated cholesteric mixture with a relatively high concentration of chiral compounds are used.

In a compensated cholesteric mixture, the helical pitch increases as the temperature is lowered towards a compensation temperature T_c at which the pitch diverges. As the temperature is lowered further the handedness of the helix reverses and the pitch again decreases. The wavevcctor close to T_c varies linearly with temperature and becomes 0 at T_c.

We have used a mixture with 35.6 mole per cent of 7P(2CN)5BC, 6.5 mole per cent of 7CB and 56 mole per cent of cholesteryl chloride. This mixture has a convenient compensation temperature and a weak positive dielectric anisotropy as required in the experiment. Using the Cano-Grandjean technique explained earlier (Chapter 11), the pitch of the helix was measured as a function of temperature.

We have shown the results on two mixtures with slightly different compositions in figures 4.14 and 4.15 respectively. It is seen from figure 4.15 that when T_c is far away from the cholesteric-isotropic transition point, q varies practically linearly with temperature. Using tlie Cano-Grandjean technique, we could riot measure pitch values larger than $\sim 35\,\mu m$. However, figures 4.14 and 4.15 show that the wavevcctor follows a smooth curve passing through 0 at T_c. The sense of the cholesteric helix was determined using the technique mentioned in chapter II. In the present case, we found that the helix was left-handed at temperatures lower than T_c and right-hatided

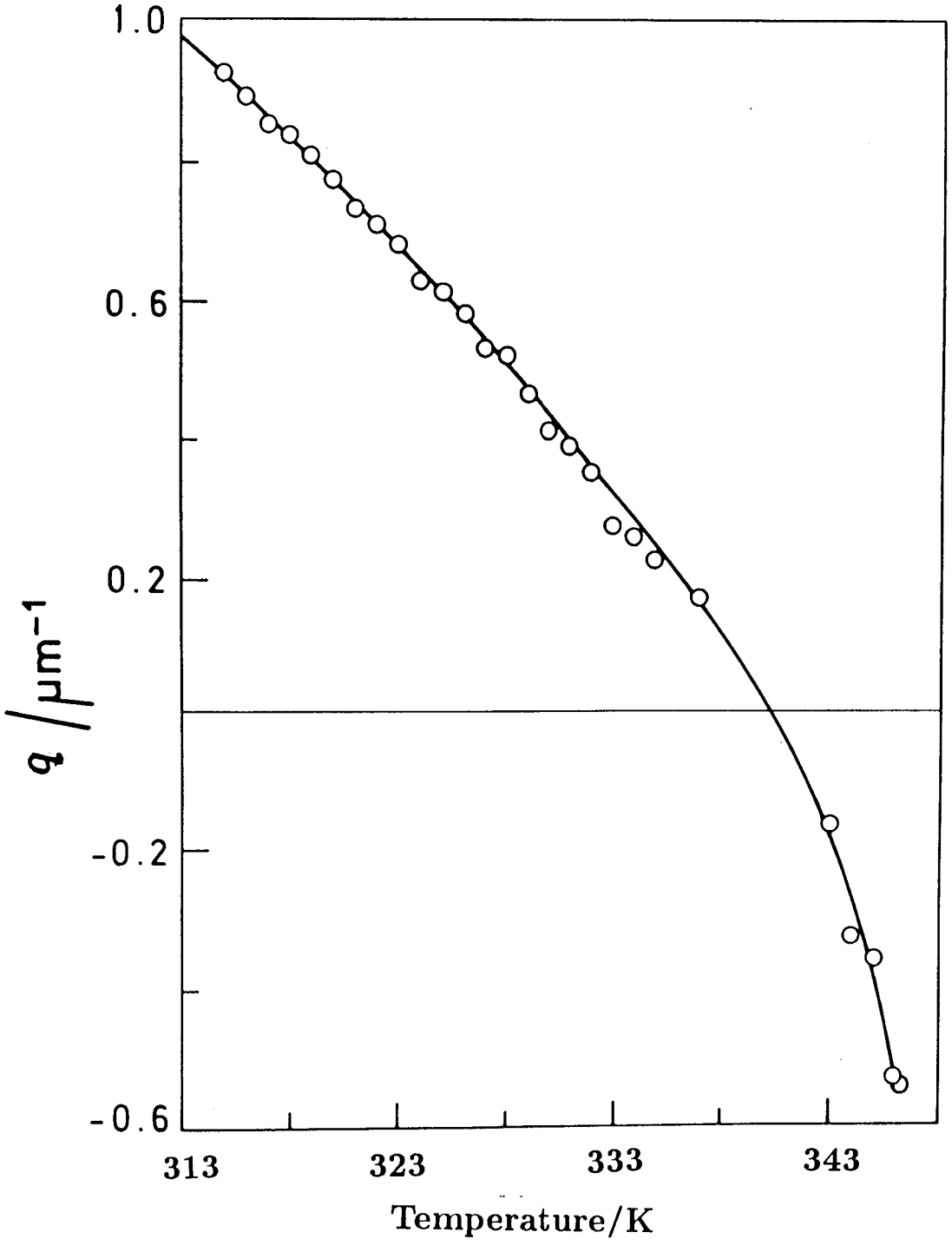

Figure 4.14. Temperature variation of wavevector q in a compensated cholesteric mixture in which T_c is only ~7° below the cholesteric-isotropic transition point, resulting in a rapid variation of q above T_c.

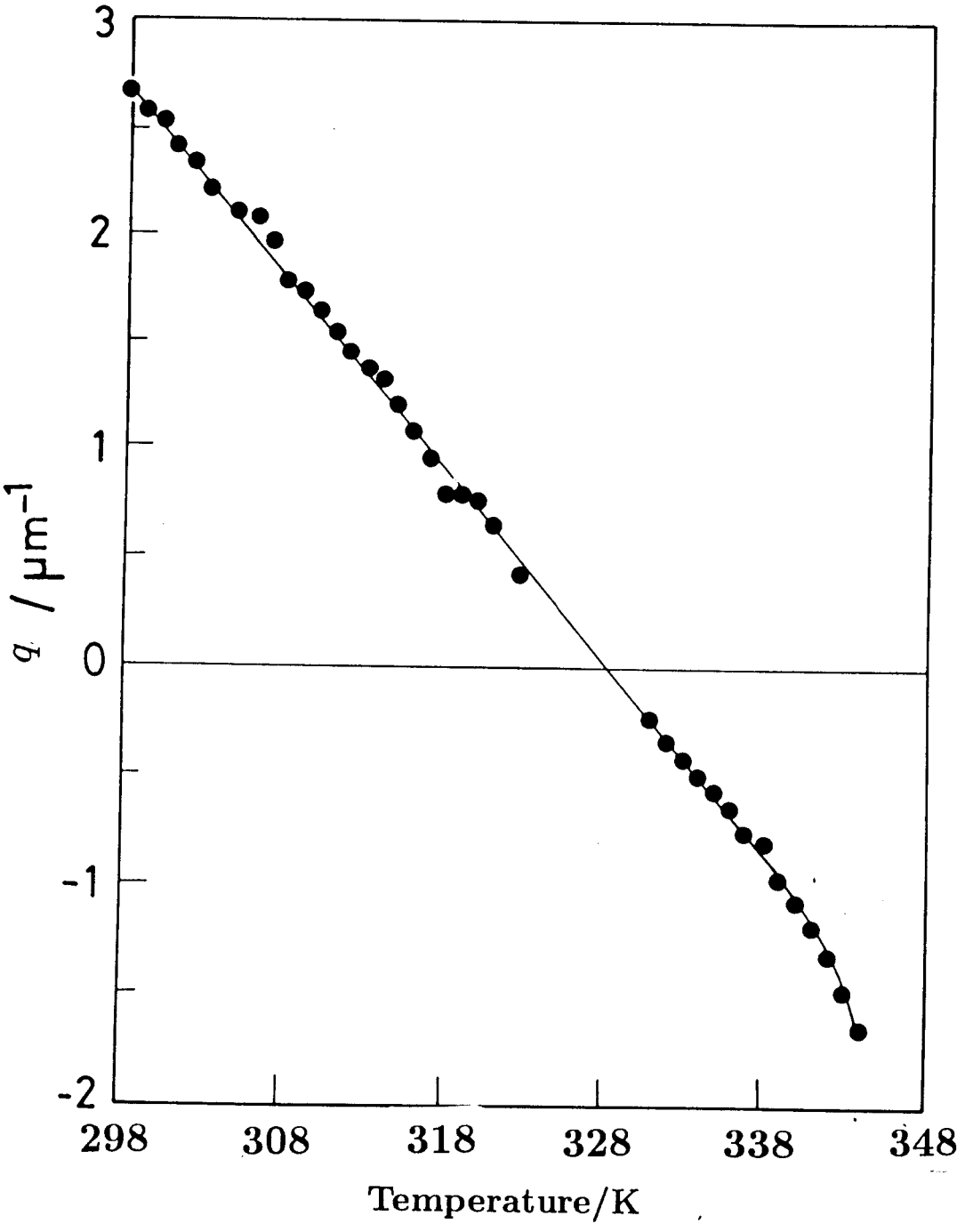

Figure 4.15. Temperature variation of wavevector q in a compensated cholesteric mixture. T_c is about 15 K below the cholesteric-isotropic transition temperature .

above T_c. The magnitude of the wavevector shows a steep increase as it approaches the cliolcstcric-isotropic transition point (Fig. 4.14).

The sample was taken in a cell with a thickness $\simeq 3\ \mu m$ and made of conductive glass plates which were treated to get a homogeneous alignment. It was slowly cooled from the isotropic phase at the rate of $\sim 0.2°/\text{min.}$ to the cholesteric pliase. Usually a number of disclination lines which segregate regions of different values of the pitch are seen in the field of view as the pitch varies rapidly even for a small change in temperature. These disclination lines seem to originate near the eclge of the sample. We could find a large enough area free of such disclinations on some rare occasions. Such an area was used in the electromechanical experiment. To avoid tlie occurrence of striped domains on application of tlie electric field above a threshold value, we choose the sample thickness to be quite small ($\simeq 3\ \mu m$) (Chigrinov et al., 1979; Cohen et al., 1990). The RMS value of the Freedericksz threshold for this sample was found to be $\simeq 1.2$ V. We found it convenient to record the electromechanical signal at an RMS voltage = 2.8 V. We made the measurements at a few different frequencies of the applied sinusoidal electric field. We measured tlie f and 2f signals and their phase angles as the temperature was lowered across the compensation temperature. A few different frequencies were used to take tlie readings at each temperature. The results of a preliminary measurement at two frequencies, viz., 17 and 37 Hz are shown in figures 4.16 arid 4.17. The magnitude of the f signal decreases and tlie phase angle of the signal increases as the temperature approaches the compensation temperature T_c. The signal again increases but with the opposite phase angle as we cross T_c (figure 4.17). The phase angle decreases in magnitude as the temperature is further lowered. But the amplitude of the signal increases. This is in accord with tlie theoretical calculations made in chapter 111 (see

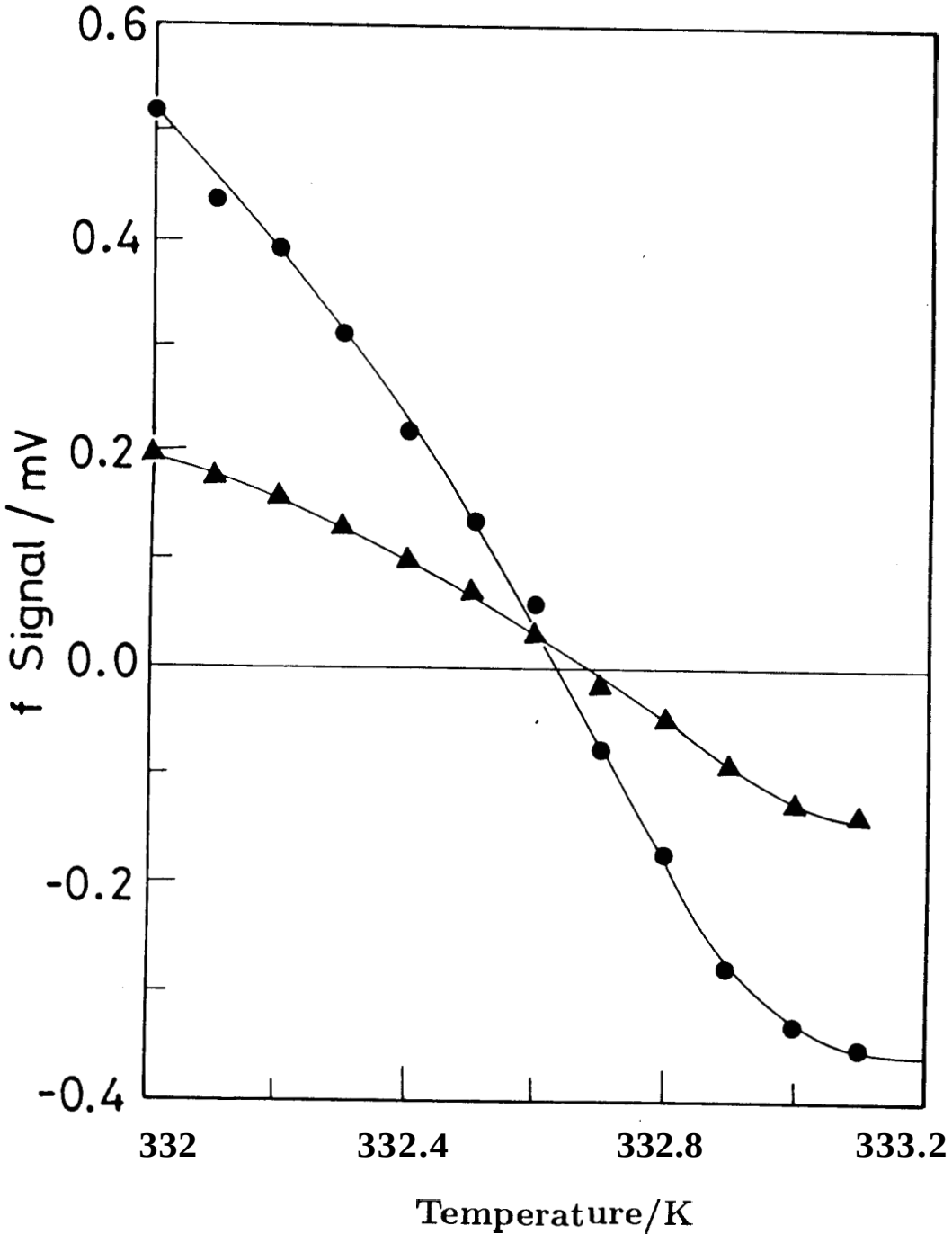

Figure **4.16.** Temperature variations of the f signals at 17 Hz (●) and 37 Hz (A) in a compensated cholesteric. The small difference in T_c between the two frequencies arises because of a more efficient heating due to ionic current at 17 Hz.

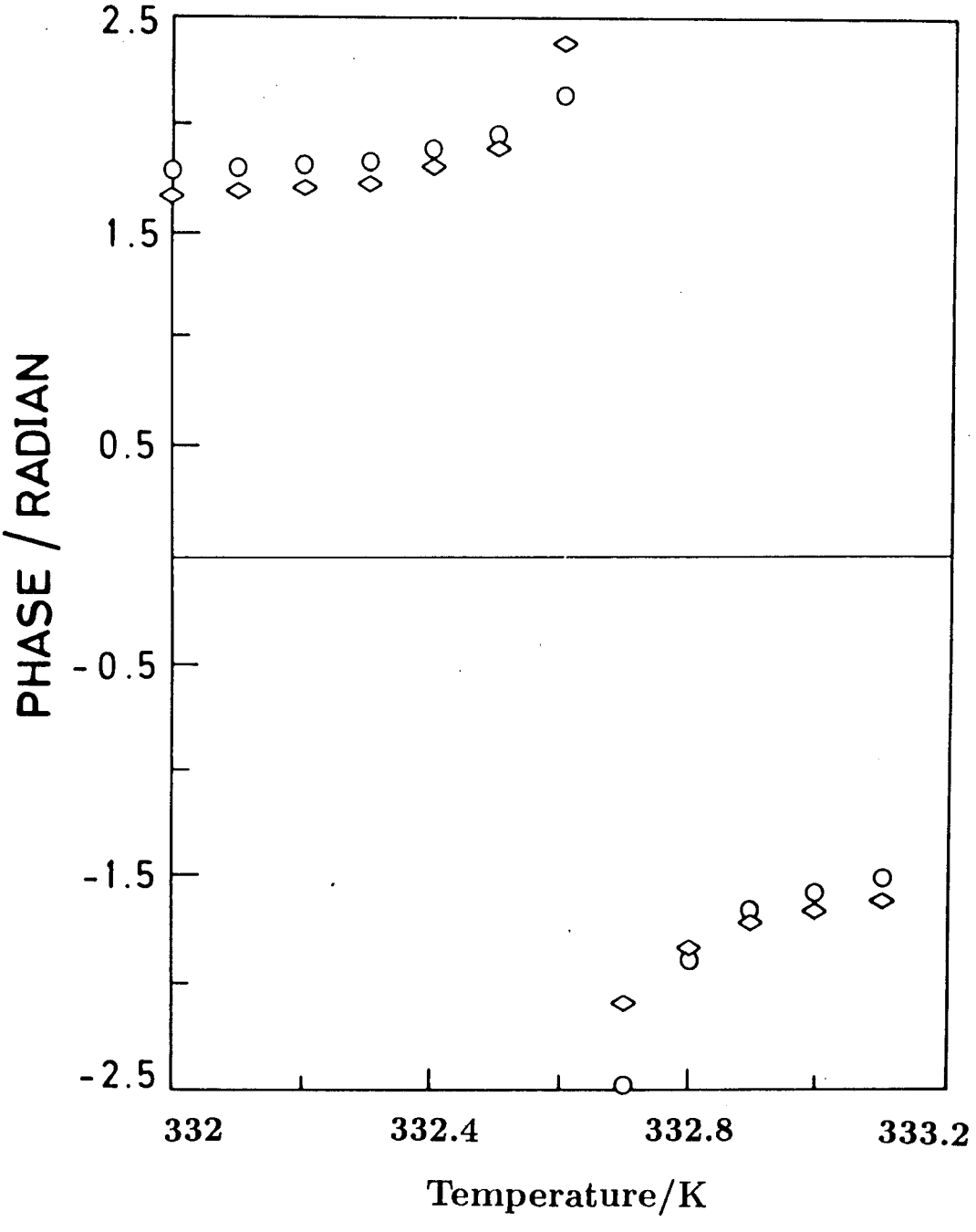

Figure 4.17. Temperature variations of the phase angles of the f signal at 17 Hz (O) and 37 Hz (O).

Fig.3.11). This signifies that the electromechanical coupling coefficient goes to zero and changes sign as we cross T_c. Another significant fact is that the signal at 17 Hz goes to zero at a slightly lower temperature (by $\sim 0.05'$) compared to the signal at 37 Hz. This phenomenon occurs probably because of greater ion flow when the field is applied at a lower frequency and the consequent additional heating of the sample, thus altering the true temperature of the sample from the measured value.

The amplitudes of the 2f signals for 17 Hz and 37 Hz have been plotted in figure 4.18. The diagram indicates that for both 17 Hz and 37 Hz, the 2f signal becomes a maximum at T_c hut the phase angle is practically independent of temperature. The origin of this maximum may be attributed to the absence of twist distortions in tlie sample with $q = 0$, i.e., at T_c. The effective Freedericksz threshold is comparatively higher when $q \neq 0$, than when $q = 0$. Because the threshold is lower for $q = 0$, the θ-oscillations in that case have a larger amplitude even though we have applied a constant voltage of 2.8 volts at all temperatures. Our experiments indicate that the threshold voltage is ~ 0.07 V lower close to T_c compared to the value at $\sim T_c + 0.5°C$.

A more detailed measurement of the electromechanical signal at five different frequencies, viz., 7, 17, 27, 37 and 57 I-Iz were also made as the temperature was increased across T_c. The results are shown in figure 4.19. We can again notice the change of sign of the electromechanical signal as the temperature is varied across T_c. We can also see clearly that the signal becomes smaller as the frequency of tlie applied electric field increases. As the temperature of the sample is increased, the electromechanical signal tends to vary more slowly. This slower variation may be due to tlie dependence of all the physical parameters like tlie dielectric anisotropy, elastic constants, viscosity, etc., on temperature. The variation of the signal close to T_c is linear. The slope of this linear part is approximately inversely proportional

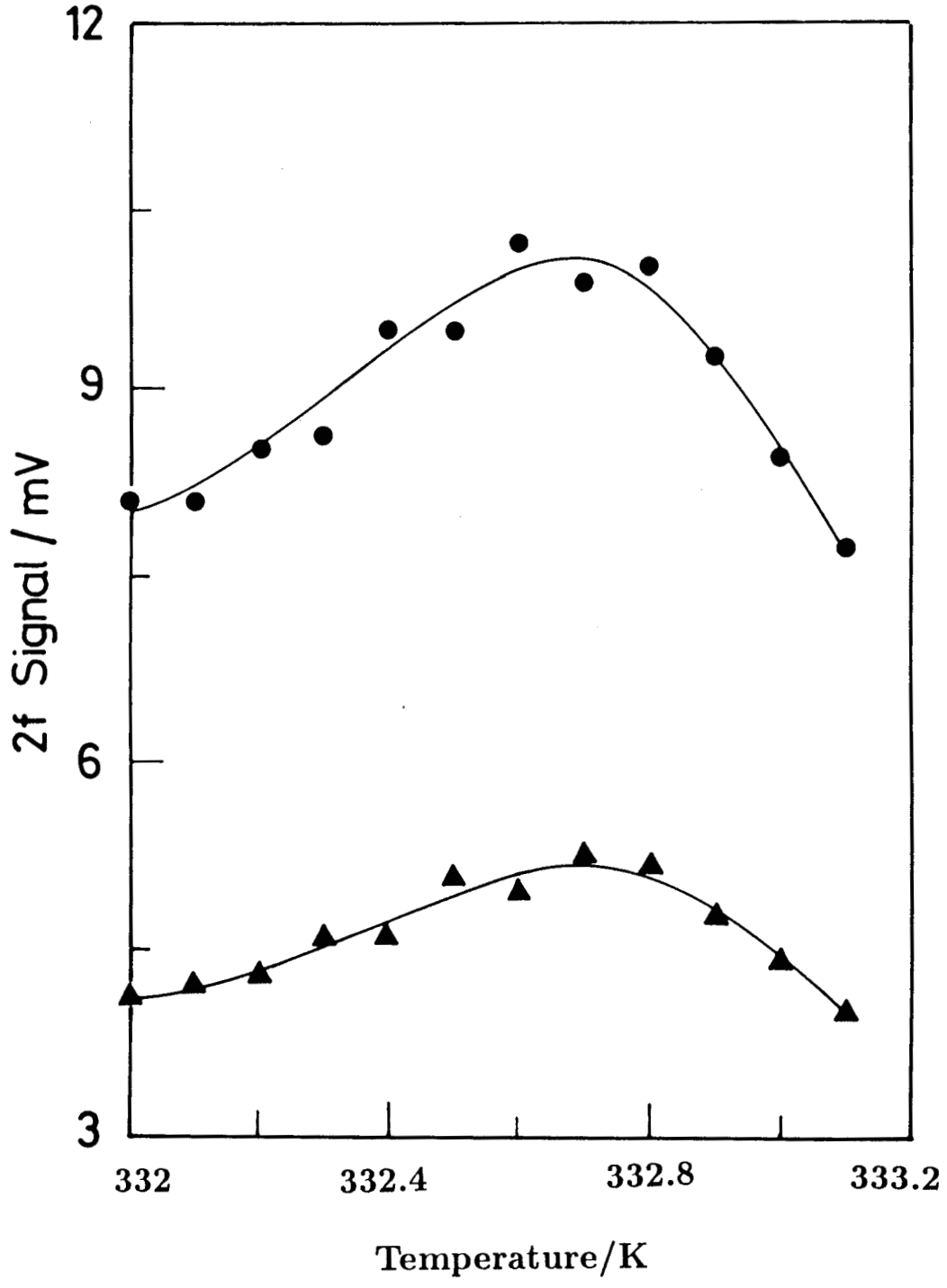

Figure 4.18. Temperature variations of the 2f signals at 17 Hz (●)and 37 Hz (▲).

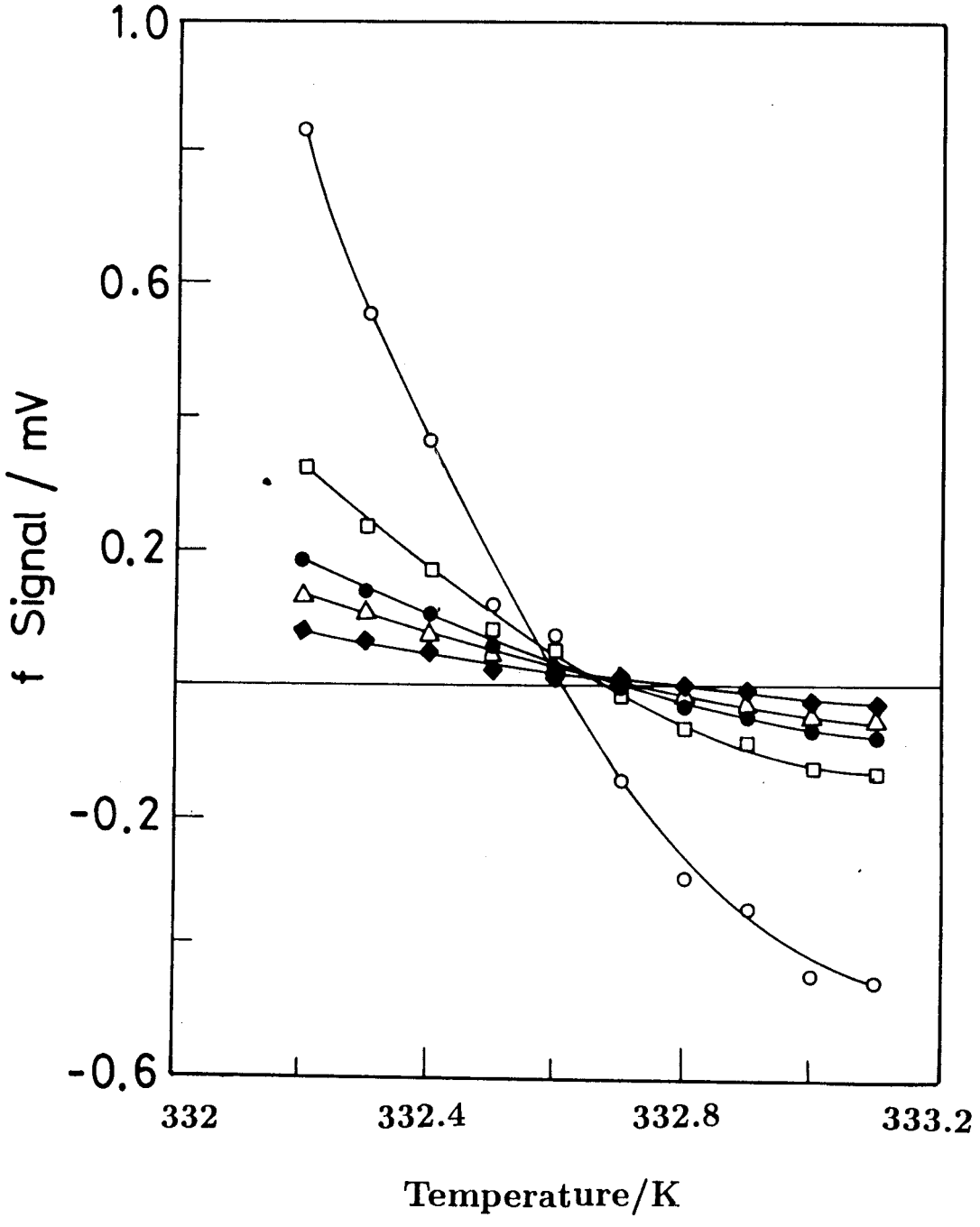

Figure 4.19. Temperature variations of the f signal at 7 Hz (O), 17 1-12 (□), 27 Hz (●), 37 Hz (A) and 57 Hz (◆).

to the frequency ($\sim \pm 20\%$), as expected from theory (see equation **3.7).**

Thus our experimental result on the compensated cliolesteric mixture again shows that the electromechanical coupling coefficient essentially depends on the *macroscopic chirality* of the cholesteric medium. The molecular contribution if any is extrerriely small and our measurements are not sensitive enough to detect such a contribution, even in this case with a high content of chiral molecules.

References

BOLYLEV,Yu.P., and PIKIN,S.A., 1977, *Sov.* Phys. JETP, 45, 195.

CHANDRASEKHAR,S., 1977, Liquid Crystals (Cambridge University Press).

CHIGRINOV,V.G., BELYAYEV,V.V., BELYAYEV,S.V. and GREBENKIN,M.F., 1979, *Sov. Phys. JETP*, 50, 994.

COHEN,G. and HORNREICH,R.M., 1990, Phys. *Review A, 41,* 8, 4402.

DE GENNES, P.G., 1975, *The Physics of* Liquid Crystals (Clarendon Press, 1975).

MADHUSUDANA,N.V. and PRATIBHA,R., 1989, Liquid Crystals, 5, 1827

SRIKANTA,B.S. and MADHUSUDANA,N.V., 1983, Mol. *Cryst.* Liquid *Cryst.*, 103,111.